



Cite this: *CrystEngComm*, 2015, 17, 281

Received 24th May 2014,
Accepted 18th July 2014

DOI: 10.1039/c4ce01073f

www.rsc.org/crystengcomm

Crystals for sustainability – structuring Al-based MOFs for the allocation of heat and cold†

M. F. de Lange,^{*ab} C. P. Ottevanger,^a M. Wiegman,^a T. J. H. Vlugt,^b J. Gascon^{*a} and F. Kapteijn^a

Several Al-based MOFs of the CAU family have been investigated for application in the adsorption driven allocation of heat and cold. The special water adsorption behaviour of CAU-10-H makes it ideal for application in adsorption driven heat pumps and chillers. For increased performance, CAU-10-H crystals have been grown directly on both γ -alumina and metallic aluminium. Crystal growth on these surfaces can be controlled by the addition of acids.

In combating global warming, reduction of the energy consumption associated with the allocation of heat and cold is of great importance. In the Netherlands, *e.g.*, roughly 38% of primary energy was consumed for these purposes, a total of 1.3×10^{18} J in 2010,¹ the majority of which was generated by fossil fuels. In order to reduce CO₂ emissions, a transition to low-grade waste thermal energy, solar or geothermal energy for heat and cold allocation is thus highly desirable. This can be achieved with adsorption driven heat pumps (AHPs) and chillers (ADCs). These devices, pioneered by Faraday in 1848,² are based on reversible adsorption and desorption of a working fluid,^{2,3} instead of conventional vapor-compression. Additionally, when H₂O is used as a working fluid, AHPs/ADCs are intrinsically environmentally benign, a clear improvement over CFCs/HFCs used in the vapor-compression counterparts. The heart of an AHP or ADC is the solid adsorbent, conventionally some type of zeolite or silica gel. In recent years however, metal-organic frameworks (MOFs) have gained increasing attention in this field,^{3–7} because of their tunable adsorption behavior and high loading capacity. For an acceptable operation window, a sorbent for AHPs/ADCs should adsorb a significant amount of H₂O at $0.05 \leq p/p_o \leq 0.3$ –0.35.^{3,8,9} Furthermore, the adsorption

isotherm should ideally have an s-shape and be devoid of hysteretic behaviour, to enable desorption at low temperatures.⁸ Obviously, the material should be stable and not degrade when subjected to H₂O. This is not a trivial requirement, as many MOFs degrade under (prolonged) exposure to water.^{10–14} Last but not least, once an interesting adsorbent has been identified, heat and mass transfer from and to the adsorbent should be optimized at the device level in order to realize a high specific power (W g^{−1}). In the case of zeolites, the use of coatings results in an improved performance over a packed bed (pellets),^{15–18} because of superior heat transfer. In the case of MOFs, deduced from scarce information on their thermal conductivity,^{19,20} it is likely that heat transfer will be a limiting factor as well. Thus, for application in AHPs/ADCs, it is highly desirable that the chosen material can be deposited on a heat exchanger-surface. Because of its natural abundance and low toxicity, aluminium would be a cost-effective metal to be used both as a heat conducting surface and as a metal-source for the MOF to be grown on. Recently, novel Al-based MOFs have been reported by Stock *et al.*,^{21–26} which have been investigated for application in adsorption-driven heat pumps in this communication. A series of potentially interesting CAU materials (CAU stands for Christian-Albrechts-Universität) were initially screened. In the second step, the most interesting adsorbent, based on its H₂O adsorption isotherm, was interfaced on Al-based substrates. From the available Al-based CAUs, CAU-3 and CAU-6 were excluded *a priori* due to their high hydrophobicity and hydrophilicity, respectively.^{25,26} CAU-1, CAU-1-(OH)₂, CAU-8, CAU-10-H, CAU-10-NH₂ and CAU-10-OH were synthesized successfully following synthesis protocols described elsewhere (see the ESI† for experimental details and characterization).^{21–24}

The H₂O adsorption isotherms of these materials are depicted in Fig. 1. Clearly, CAU-1, containing octameric [Al₈(OH)₄(OCH₃)₈]¹²⁺ clusters connected with 2-aminoterephthalic acid ligands, displays a beneficial s-shaped isotherm, but the amount adsorbed at $p/p_o \leq 0.35$ is rather low. When the organic ligand is changed to 2,5-hydroxyterephthalic acid

^a Catalysis Engineering, Chemical Engineering Department, Delft University of Technology, Julianalaan 136, 2628 BL Delft, the Netherlands.

E-mail: M.F.deLange@tudelft.nl, j.gascon@tudelft.nl

^b Engineering Thermodynamics, Process & Energy laboratory, Delft University of Technology, Leeghwaterstraat 39, 2628 CB Delft, the Netherlands

† Electronic supplementary information (ESI) available: Experimental conditions and characterization of various CAU samples (powder) and CAU-10-H on various supports (α -alumina, γ -alumina, aluminium). See DOI: 10.1039/c4ce01073f





Fig. 1 H₂O adsorption isotherms at 298 K of CAU-1 (■), CAU-1-(OH)₂ (●), CAU-8 (▲), CAU-10-H (▼), CAU-10-NH₂ (◆) and CAU-10-OH (◄).

(CAU-1-(OH)₂), adsorption is moderately higher for $p/p_0 \leq 0.35$, but the undesired inclination of adsorption at low p/p_0 would require an undesirably high temperature in the desorption step. CAU-8, consisting of [Al-OH]²⁺ chains connected through 4,4'-benzophenonedicarboxylic acid ligands, shows a very particular adsorption behaviour; the isotherm is seemingly composed of two separate type III isotherms (IUPAC-classification).^{27,28} The low uptake at $p/p_0 \leq 0.35$, however, renders it of little use for the application at hand. On the other hand, the very narrow step in p/p_0 for CAU-10-H, comprised of [Al-OH]²⁺ chains linked together by isophthalic acid, makes it an ideal material for the target application. Functionalization of this framework with either amino- or hydroxyl-groups results in a less desired behaviour due to the inclined adsorption at low p/p_0 . Summarizing, in view of its outstanding thermal stability (Fig. S3†), its isotherm shape, its large adsorption capacity (~25 wt.%) and the absence of hysteresis, CAU-10-H is a promising adsorbent for application in the adsorption driven allocation of heat and cold. Furthermore, with an average isosteric heat of adsorption of about -54 kJ mol⁻¹ (Fig. S6†), regeneration of CAU-10-H is less energy-intensive than for the current benchmark adsorbents used in ADHs/ADCs,²⁹ and those commercialized by Mitsubishi Plastics, *e.g.* FAM Z01,³⁰ Z02 (ref. 31) and Z05.³² In comparison, CAU-10-H shows the same advantageous s-shaped isotherm as FAM Z01 and Z05, but has a higher adsorption capacity.

In order to further explore the applicability of CAU-10-H, the growth of this MOF on different surfaces was studied in detail. The procedure to create a coating of CAU-10-H, based on the work of Reboul *et al.*,³³ is to dissolve aluminium ions from the support, directing crystal growth towards the interface with the linker in solution (without adding an additional aluminium-source). In addition, to facilitate crystal growth, the effect of adding either acetic or hydrochloric acid was investigated. Both low pH and carboxylate species aid in the dissolution of metal ions from oxides.³⁴ Furthermore, carboxylic acids are commonly used as modulators in the synthesis of MOF crystals,^{35–38} and the addition of HCl has been found beneficial in the synthesis of certain MOFs.³⁹

Applying this protocol to γ -alumina beads (see the ESI† for experimental details) proved successful in forming crystals

attached to the external surface, as can be seen from the SEM images depicted in Fig. 2.

The surface coverage becomes more homogeneous when acetic acid is added and even more homogeneity is observed when HCl is used. For HCl, the surface seems to be completely covered with crystals. TGA/SDTA confirms that there is no excess of organic ligands present (Fig. S10 and S11†) and that the thermal stability of the crystals is equal to that of CAU-10-H. We speculate that the use of a non-coordinating, stronger acid is more beneficial because: (i) dissolution of Al is more efficient at lower pH and (ii) slower deprotonation of the linker and the absence of other coordinating moieties (like acetates) favours the formation of more homogeneous, smaller crystals. Furthermore, it might be that the formation of HCl-DMF complexes could have a beneficial effect on the growth kinetics, as was shown for other Al-based MOFs.⁴⁰ Assuming that, after solvent removal, all weight loss is due to decomposition of the MOF on the support, the loading of CAU-10-H would be roughly 33, 34, and 38 wt.% for the beads without acid, with acetic acid, and with HCl, respectively. XRD analysis of these beads (Fig. S11†) confirms that these crystals are CAU-10-H. The characteristic step in H₂O adsorption is also retained for these beads (Fig. S13†). Cracking a bead of CAU-10-H (HCl synthesis) showed that growth occurs exclusively on the external surface, as the interior seemed devoid of any crystals (Fig. S15†). This means in turn, that an achievable loading of such beads depends on the surface-to-volume ratio.

Syntheses on α -alumina were found to be unsuccessful (Fig. S7†). Hardly, if any, crystal growth could be observed on these supports. This is attributed to the higher stability of α -alumina compared to γ -alumina, and thus the higher resistance to acid leaching.

The promising results of CAU-10-H supported on γ -alumina serve as a starting point for further investigation, as porous metal-oxides themselves do not serve well as heat conductive

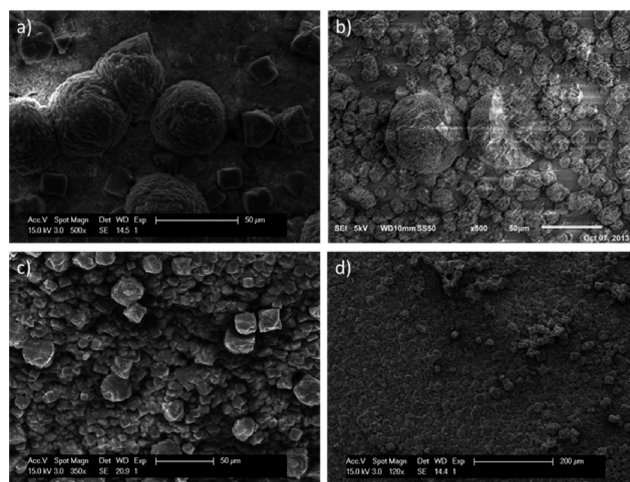


Fig. 2 SEM images of CAU-10-H synthesized on γ -alumina beads without any acid (a), with the addition of acetic acid (b) and with the addition of hydrochloric acid (c and d).



interfaces. For AHPs/ADCs, it is desired to have a MOF-layer grown directly on a metallic support. For CAU-10-H, one could opt to create a layer of Al_2O_3 on top of an aluminium surface prior to synthesis, so that the oxide-layer can be converted into MOF crystals. Here, attempts have been made to directly grow CAU-10-H crystals on top of aluminium without any pre-treatment, by extracting the metal ions required for the MOF from the support. Again, the effect of acid addition was studied (for experimental details, see the ESI†). Note that on any aluminium surface exposed to atmospheric oxygen, a natural oxide layer of around 4 nm is present.⁴¹

As indicated by the SEM images in Fig. 3, crystals are formed on the metal surface. Similar to what was found for γ -alumina beads, the introduction of acid improves coverage. This can even be concluded by regular images of the Al-support after synthesis (Fig. 3g–i). Furthermore, it seems that for the synthesis where HCl was added, there are microscopic grooves on the aluminium surface, due to the

dissolution of Al^{3+} ions. Most likely, aluminium is dissolved preferentially from the local aluminium crystal boundaries in the metallic support. Comparing the hydrochloric acid-aided syntheses of γ -alumina and metallic aluminium, the crystal size of the rhombic particles on the latter seems larger, and there are more crystal agglomerates. Future endeavours should be directed to optimizing further homogeneous crystal growth on the surface. XRD confirms the presence of CAU-10-H (Fig. S17†), albeit that there seems to be a minor reflection contribution of an unknown secondary crystal phase, also observed when HCl is added to the bulk synthesis of CAU-10-H (Fig. S18†). During the experiments leading to the discovery of CAU-10-H, it was stated that a secondary phase was observed for the molar ratio of Al^{3+} :ligand > 3, however no characterization of this secondary phase was given for comparison.²⁴

To assess the adsorptive capacities of the CAU-10-H coating, the hydrochloric acid-aided synthesis was repeated on an aluminium plate that was *a priori* rolled into a cylindrical shape, to make the resulting coating measurable in a volumetric adsorption set-up. Subsequently, five water adsorption and desorption measurements were performed, as depicted in Fig. 4.

The shape of the adsorption isotherm of CAU-10-H coated on aluminium is strikingly similar to that of the bulk-phase (Fig. 1). The only minor difference is the stronger inclination of adsorbed water at $p/p_0 > 0.2$, after the steep step in water uptake. Furthermore, an observed closure of the desorption loop at $p/p_0 \sim 0.35$, not attributable to the CAU-10-H structure, is likely to be due to water condensation in the mesopores.⁴² Whether the mesoporosity is caused by the secondary phase observed or by condensation of water in inter-particle spaces is unclear. More importantly, there is no desorption hysteresis in the region of the large step in water uptake, a feature highly desirable for the target application. Furthermore, these measurements indicate clearly that there is no loss of capacity, as the adsorption behaviour is identical



Fig. 3 SEM images of CAU-10-H synthesized directly on metallic aluminium both without using any additional acid during synthesis (a and b), using acetic acid (c and d) and using hydrochloric acid (e and f), for 100 \times magnification (a, c and e, scale bar indicates 100 μm) and 300 \times magnification (b, d and f, scale bar indicates 50 μm). Photographs of (2 by 2 cm) aluminium plates after synthesis without acid (g), with acetic acid (h) and with hydrochloric acid (i).

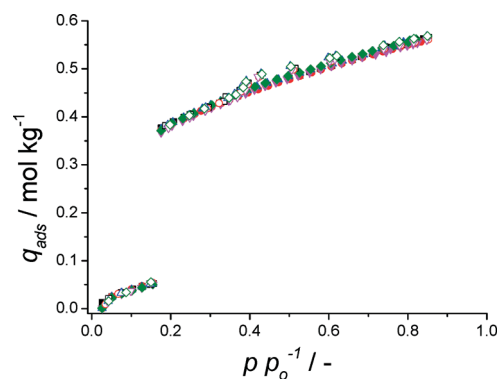


Fig. 4 Repeated H_2O adsorption isotherms at 298 K of CAU-10-H supported on a metallic aluminium plate. First (■), second (●), third (▲), fourth (▼) and fifth (◆) measurements. Closed symbols depict adsorption, open desorption. Loading is presented as per total mass of sample (Al substrate + CAU-10-H).



for all measurements. This means that the coated CAU-10-H is perfectly stable, at least for 5 cycles of adsorption and desorption of water.

Note that the quantity adsorbed is based on the total mass of the sample (MOF and aluminium plate). Due to the synthetic procedure and the fact that both the substrate and MOF contain aluminium, direct quantification of the loading of CAU-10-H turned out to be difficult. As MOF crystals are grown on a flat metal surface rather than in a porous medium, expressing the content of MOF as a (weight) fraction relative to bulk aluminium would not yield a representative figure of merit. These measurements however, do indicate that up to 38 kJ of heat can be withdrawn in the evaporator of an AHP/ADC per square meter of coated aluminium surface.

Conclusions

Of the aluminium-based Metal–Organic Frameworks (MOFs) investigated for application in adsorption driven heat pumps (AHPs) and chillers (ADCs), CAU-10-H was shown to have ideal adsorptive properties. Growth of CAU-10-H crystals directly on γ -alumina supports was achieved by using aluminium ions from the substrate as the metal source for the MOF. Addition of acids improves the growth of these crystals. In particular hydrochloric acid has a beneficial effect on surface coverage and homogeneity of the formed crystal size and shape. The same approach was successfully applied to coat CAU-10-H directly on metallic aluminium, which is highly desired for the target application. Again HCl has a beneficial effect on crystal growth. The adsorptive properties of CAU-10-H are similar to that of the bulk material and the coating was shown to be stable in at least 5 water adsorption–desorption cycles.

Acknowledgements

Financial support from the Advanced Dutch Energy Materials (ADEM) program of the Dutch Ministry of Economic Affairs, Agriculture and Innovation is gratefully acknowledged.

Notes and references

- National Expertisecentrum Warmte, 2013.
- R. Critoph and Y. Zhong, *P. I. Mech. Eng. E-J. Pro.*, 2005, **219**, 285–300.
- S. K. Henninger, F. Jeremias, H. Kummer and C. Janiak, *Eur. J. Inorg. Chem.*, 2011, **4**, 471–474.
- S. K. Henninger, H. A. Habib and C. Janiak, *J. Am. Chem. Soc.*, 2009, **131**, 2776–2777.
- C. R. Wade, T. Corrales-Sanchez, T. C. Narayan and M. Dincă, *Energy Environ. Sci.*, 2013, **6**, 2172–2177.
- G. Akiyama, R. Matsuda and S. Kitagawa, *Chem. Lett.*, 2010, **39**, 360–361.
- G. Akiyama, R. Matsuda, H. Sato, A. Hori, M. Takata and S. Kitagawa, *Microporous Mesoporous Mater.*, 2012, **157**, 89–93.
- Y. I. Aristov, *Appl. Therm. Eng.*, 2013, **50**, 1610–1618.
- M. Wickenheisser, F. Jeremias, S. K. Henninger and C. Janiak, *Inorg. Chim. Acta*, 2013, **407**, 145–152.
- J. J. Low, A. I. Benin, P. Jakubczak, J. F. Abrahamian, S. A. Faheem and R. R. Willis, *J. Am. Chem. Soc.*, 2009, **131**, 15834–15842.
- P. M. Schoenecker, C. G. Carson, H. Jasuja, C. J. J. Flemming and K. S. Walton, *Ind. Eng. Chem. Res.*, 2012, **51**, 6513–6519.
- P. Kusgens, M. Rose, I. Senkovska, H. Frode, A. Henschel, S. Siegle and S. Kaskel, *Microporous Mesoporous Mater.*, 2009, **120**, 325–330.
- K. A. Cychosz and A. J. Matzger, *Langmuir*, 2010, **26**, 17198–17202.
- F. Jeremias, V. Lozan, S. K. Henninger and C. Janiak, *Dalton Trans.*, 2013, **42**, 15967–15973.
- G. Restuccia, A. Freni and G. Maggio, *Appl. Therm. Eng.*, 2002, **22**, 619–630.
- L. Bonaccorsi, P. Bruzzaniti, L. Calabrese, A. Freni, E. Proverbio and G. Restuccia, *Appl. Therm. Eng.*, 2013, **61**, 848–852.
- B. Dawoud, *Appl. Therm. Eng.*, 2013, **50**, 1645–1651.
- M. Tatlier, B. Tantekin-Ersolmaz and A. Erdem-Şenatalar, *Microporous Mesoporous Mater.*, 1999, **27**, 1–10.
- B. L. Huang, Z. Ni, A. Millward, A. J. H. McGaughey, C. Uher, M. Kaviani and O. Yaghi, *Int. J. Heat Mass Transfer*, 2007, **50**, 405–411.
- D. Liu, J. Purewal, J. Yang, A. Sudik, S. Maurer, U. Mueller, J. Ni and D. Siegel, *Int. J. Hydrogen Energy*, 2012, **37**, 6109–6117.
- T. Ahnfeldt, N. Guillou, D. Gunzelmann, I. Margiolaki, T. Loiseau, G. Férey, J. Senker and N. Stock, *Angew. Chem., Int. Ed.*, 2009, **48**, 5163–5166.
- T. Ahnfeldt, J. Moellmer, V. Guillermin, R. Staudt, C. Serre and N. Stock, *Chem. – Eur. J.*, 2011, **17**, 6462–6468.
- H. Reinsch, M. Krüger, J. Marrot and N. Stock, *Inorg. Chem.*, 2013, **52**, 1854–1859.
- H. Reinsch, M. A. van der Veen, B. Gil, B. Marszalek, T. Verbiest, D. de Vos and N. Stock, *Chem. Mater.*, 2012, **25**, 17–26.
- H. Reinsch, M. Feyand, T. Ahnfeldt and N. Stock, *Dalton Trans.*, 2012, **41**, 4164–4171.
- H. Reinsch, B. Marszalek, J. Wack, J. Senker, B. Gil and N. Stock, *Chem. Commun.*, 2012, **48**, 9486–9488.
- K. Sing, D. Everett, R. Haul, L. Moscou, R. Pierotti, J. Rouquerol and T. Siemieniowska, *Pure Appl. Chem.*, 1982, **54**, 2201.
- R. Pierotti and J. Rouquerol, *Pure Appl. Chem.*, 1985, **57**, 603–619.
- M. Goldsworthy, *Microporous Mesoporous Mater.*, 2014, **196**, 59–67.
- H. Kakiuchi, S. Shimooka, M. Iwade, K. Oshima, M. Yamazaki, S. Terada, H. Watanabe and T. Takewaki, *Kagaku Kogaku Ronbunshu*, 2005, **31**, 361–364.



- 31 H. Kakiuchi, S. Shimooka, M. Iwade, K. Oshima, M. Yamazaki, S. Terada, H. Watanabe and T. Takewaki, *Kagaku Kogaku Ronbunshu*, 2005, **31**, 273–277.
- 32 S. Shimooka, K. Oshima, H. Hidaka, T. Takewaki, H. Kakiuchi, A. Kodama, M. Kubota and H. Matsuda, *J. Chem. Eng. Jpn.*, 2007, **40**, 1330–1334.
- 33 J. Reboul, S. Furukawa, N. Horike, M. Tsotsalas, K. Hirai, H. Uehara, M. Kondo, N. Louvain, O. Sakata and S. Kitagawa, *Nat. Mater.*, 2012, **11**, 717–723.
- 34 W. Stumm and R. Wollast, *Rev. Geophys.*, 1990, **28**, 53–69.
- 35 A. Schaate, P. Roy, A. Godt, J. Lippke, F. Waltz, M. Wiebcke and P. Behrens, *Chem. – Eur. J.*, 2011, **17**, 6643–6651.
- 36 H. Guo, Y. Zhu, S. Wang, S. Su, L. Zhou and H. Zhang, *Chem. Mater.*, 2012, **24**, 444–450.
- 37 J. M. Chin, E. Y. Chen, A. G. Menon, H. Y. Tan, A. T. S. Hor, M. K. Schreyer and J. Xu, *CrystEngComm*, 2013, **15**, 654–657.
- 38 A. Morsali and M. A. Alavi, *CrystEngComm*, 2014, **16**, 2246–2250.
- 39 M. J. Katz, Z. J. Brown, Y. J. Colón, P. W. Siu, K. A. Scheidt, R. Q. Snurr, J. T. Hupp and O. K. Farha, *Chem. Commun.*, 2013, **49**, 9449–9451.
- 40 M. G. Goesten, P. C. Magusin, E. A. Pidko, B. Mezari, E. J. Hensen, F. Kapteijn and J. Gascon, *Inorg. Chem.*, 2014, **53**, 882–887.
- 41 T. Campbell, R. K. Kalia, A. Nakano, P. Vashishta, S. Ogata and S. Rodgers, *Phys. Rev. Lett.*, 1999, **82**, 4866–4869.
- 42 M. Thommes, S. Mitchell and J. Pérez-Ramírez, *J. Phys. Chem. C*, 2012, **116**, 18816–18823.

